SESAME STORAGE RING BEAM DYNAMICS IN VIEW OF THE RESULTS OF ITS MAGNETS MEASUREMENTS

M. Attal, E. Huttel, SESAME, P.O.Box 7, Allan 19252, Jordan

Abstract

SESAME storage ring magnets have been recently constructed and measured. The storage ring beam dynamics is reviewed in this article in view of these results. Moreover it is shown how the optical impact of dipoles main field errors is more mitigated by sorting dipoles in the storage ring in addition to the alignment optimization method suggested by magnetic measurement outcome.

INTRODUCTION

SESAME storage ring composes 16 cells with one curved parallel-face dipole, 4 quadrupoles and 4 sextupoles in each. The vertical focusing is done mainly by the dipole gradient in addition to two auxiliary short defocusing quadrupoles used for more optical flexibility. The sextupoles accommodate also the orbit correctors and skew quadrupole coils. The 16 one-family dipoles are powered by one power supply, whereas each one of the two-family quadrupoles is powered by independent power supply, and the two-family sextupoles are powered by 4 power supplies. In SESAME machine, the beam is injected into storage ring at 800 MeV then ramped up to the operational energy 2.5GeV. SESAME storage ring magnets have been recently fabricated and measured [1] in the framework of theCESSAMag project , a SESAME-CERN/EU collaboration [2]. The dipole measurement results obtained without corrected position are called '*as delivered*'[1]. Then a scheme of dipole displacements and rotations has been suggested, in order to reduce the main measured field errors. Its corresponding results are called '*optimized alignment*' [1]. In general the measured main field errors and high order multipoles are well within the machine tolerances [3, 4] except skew field components in the dipoles which are reduced later by the '*optimized alignment*' scheme. The next sections discuss measurement results of each type of the storage ring magnets and their impact on SESAME beam dynamics.

BENDING MAGNETS

Main parameters of the design hard-edge dipole magnet at top energy are listed in Table 1. The *as delivered* measured relative deviations in dipoles integrated flux and gradient from design values at top and injection energies are shown in Fig. 1. The measured rms relative error in integrated flux $\Delta(\int Bdl) / (\int Bdl)_{av} = 1.4e^{-3}$ is within the tolerance limit $2e^{-3}$[3] where $(\int Bdl)_{av}$, the average measured value all over the 17 dipoles, is almost equal to the design value too. The most flux-deviated dipole number 7 is excluded from the main storage ring dipoles and considered as a spare one.

Table 1: Design Parameters of Storage Ring Dipole

Parameter	Symbol	Value
Magnetic length (m)	L_0	2.2500
Main flux (T)	B_0	1.4554
Main gradient (T/m)	G_0	-2.7943
Bending angle (deg)	θ	22.500
Total integrated gradient (T)	∫G.L	-6.8661

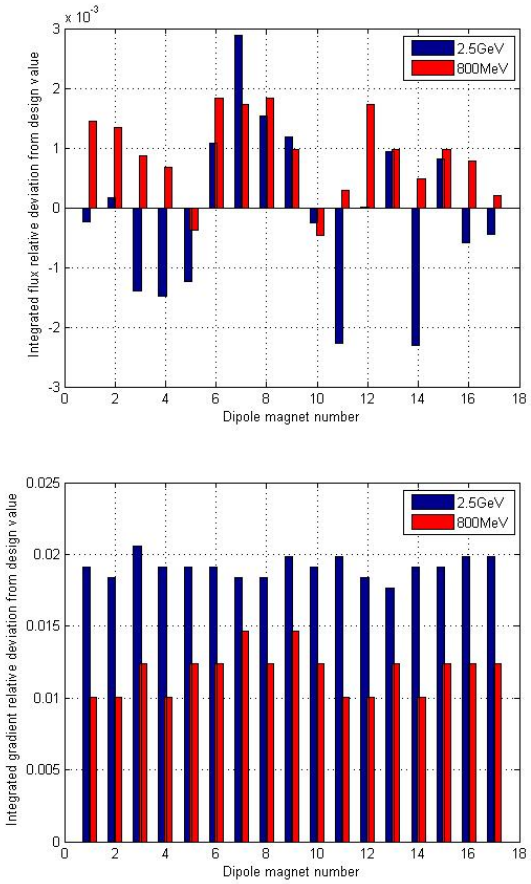

Figure 1: The *as delivered* measured deviations in dipoles integrated flux (top) and absolute integrated gradient (bottom) from design values at top and injection energies.

The nominal values of measured flux B and gradient G in each dipole are considered as the average values over -

0.6 m ≤ *s* ≤ 0.6 m, where *s* is the coordinate along the particle trajectory.

Sorting Dipoles in the Storage Ring

The dipoles integrated flux errors result in closed orbit distortion whose amplitude depends on the error values and the phase advance between them. So to reduce the orbit distortion either error values should be reduced or phase between them should be optimized by doing a specific arrangement for their hosting dipoles in the storage ring using a method called *sorting* [5]. The first option could be achieved by the *optimized alignment* scheme resulting in $\Delta(\int Bdl) / (\int Bdl)_{av} = 5e^{-5}$. However this was done only for the top energy case causing integrated flux errors at injection energy to be even larger. So it was foreseen to use both *sorting* and *optimized alignment* methods. The correlation existing between flux errors at top and injection energies made sorting at top energy valid also at injection energy. It was foreseen also not to include dipole gradient errors into the sorting process since these errors can be easily compensated for using the independently powered quadrupoles.

The dipole sorting was done by changing randomly the dipole flux error distribution in storage ring each time and calculating the total value of Courant-Snyder parameter $\varepsilon = \gamma x^2 + 2\alpha x x' + \beta x'^2$ of the created closed orbit, which was used as the cost function, all over the ring. The minimum value obtained for Courant–Snyder parameter represents the least orbit distortion which corresponds in turn to the best dipole distribution in storage ring among the tried 20,000 options. The minimum ε was $1.54e^{-6}$ m.rad whereas the maximum ε was $1.38e^{-4}$ m.rad as calculated using Accelerator Toolbox [6]. The closed orbit distortions of sorted and alignment-optimized dipoles at top and injection energies are shown in Fig. 2.

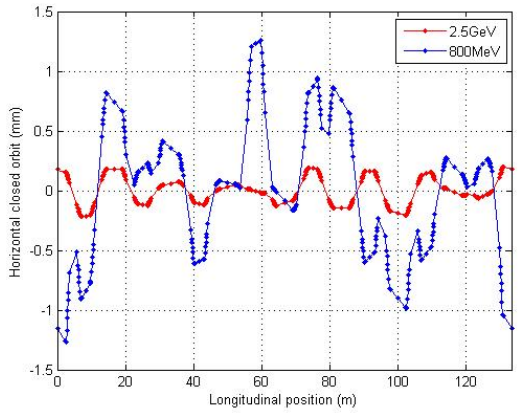

Figure 2: Closed orbit distortions obtained by adopting sorting and optimized alignment methods.

Dipoles Gradient Errors

CERN had selected a system of three blocks with different width aligned in transverse direction as inner-central-outer to be as end chamfer. The standard width of blocks chosen is 9-7-5 mm. This configuration, which was preferred for some technical reasons, however gives an average edge rotation of 7.8° compared to nominal 11.25°. Thus the total integrated gradient in dipoles is less than the design one by rms value -13%. Using different block sizes allowed correcting the gradients to get them equal within 1.5%. Changing the bloc sizes to 8-7-6 on one side reduces the edge rotation by -0.3°. The appreciable reduction in edge focusing resulted in large vertical tune shift ΔQ_y = -0.297 and large vertical beta beat as given by BETA code [7] and shown in Fig. 3.

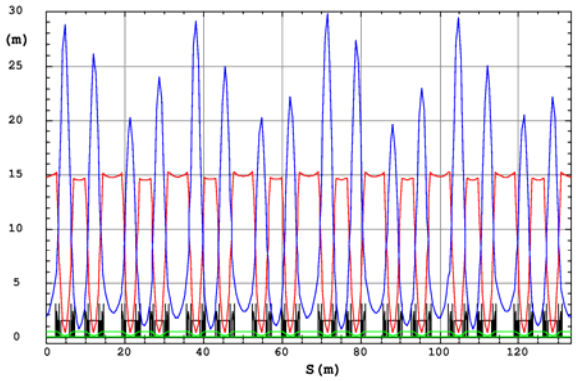

Figure 3: Optical distortion represented mainly by vertical beta beat (blue). Horizontal beta function is in red.

The reduction in total gradient and the consequent optical distortion are compensated by the defocusing quadrupoles which flank the dipole. The average and maximum relative variations in their k-values 20.4% and 32.6% are required to get back the design working point (7.23, 6.19) and set back the Twiss parameters α_x and α_y to zero in middle of each straight section. Consequently, the design dynamic aperture is recovered back without any additional optimization.

Dipole High Order Multipoles

The rms values of high order multipoles, measured at radius R = 20mm, in bending magnets are much smaller than the machine tolerance [4], whereas they are not measurable above octupole component as shown in Fig. 4. As a result the dynamic aperture is negligibly affected.

Skew Dipole and Quadrupole Components

The measured skew dipole and quadrupole components in bending magnets are that high that their optical impact is not negligible. They create a large vertical orbit distortion that makes beam rotation in the storage ring critical. However a system of washers is used to adjust both roll and vertical displacement. Maximum and rms corrections are 1.7 mm / 0.6 mrad and 0.6 mm / 0.1 mrad.

QUADRUPOLE MAGNETS

The 64 storage ring quadrupoles are divided into two types; 32 focusing quadrupoles (QF) with design magnetic length l_{qf} = 0.3 m and integrated gradient g. l_{qf} =

5 T at 2.5 GeV energy, and 32 defocusing ones (QD) with the design values l_{qd} = 0.1 m and $g.l_{qd}$ = -0.83 T.

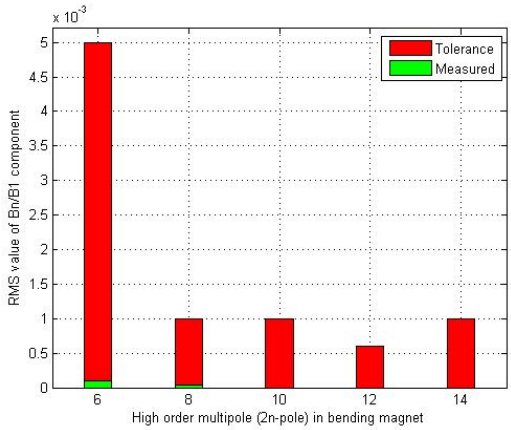

Figure 4: High order multipoles in dipole measured at R = 20mm versus tolerance values.

Main Gradient Errors

The measured rms values of gradient errors, relative to average value, dB_2/B_{2av} are $9.7e^{-4}$ in QF and $8.4e^{-4}$ in QD magnets. Although these errors are within the tolerance values $2e^{-3}$ in QF and $1e^{-2}$ in QD quadrupoles [3], nevertheless they can be compensated, if needed, using the independent power supply for each quadrupole.

High Order Multipoles

Due QF superiority in strength, the machine tolerance on quadrupole field errors is enough to be represented by its case. The normal and skew high order mutipoles, measured at radius R = 24mm, in QF quadrupoles are shown in Fig. 5 compared to the tolerance values [4]. Impact of the measured field errors on beam stability and lifetime is negligible.

Deviations of Magnetic Centres

The measured rms x, y deviations of quadrupole magnetic centres from mechanical ones in QF are dx = 0.07 mm and dy = 0.032 mm, whereas tolerance values are 0.1 mm in both planes [3, 4]. The shifts rms values can be made even smaller using 0.1 mm thick shims to minimize the errors dx, dy that are larger than 0.05 mm.

SEXTUPOLE MAGNETS

The 64 storage ring sextupole magnets have the same specifications with design magnetic length l_s = 0.1 m, but optical wise half of them is focusing with design integrated gradient $h.l_s$ = -8.81 T/m while the other half is defocusing with design $h.l_s$ = -13.9 T/m which correspond to chromaticities +5 in both planes.

Main Gradient Errors

The measured rms error in main gradients from the average value, dB_3/B_{3av} is $1.1e^{-3}$ which is much smaller than the tolerance value $1e^{-2}$ [3].

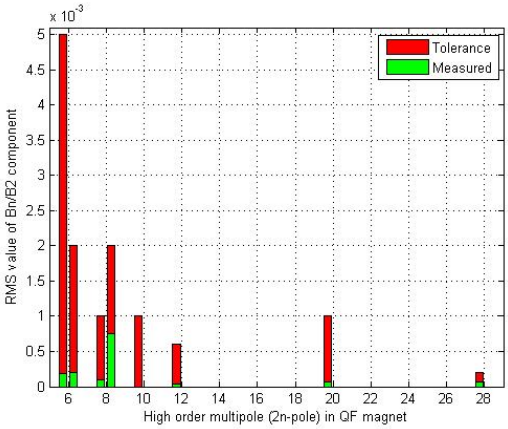

Figure 5: High order multipoles in QF quadrupole measured at R = 24mm versus tolerance values. Left bars are normal and right bars are skew components.

High Order Multipoles

Normal and skew high order multipoles, measured at R = 24mm, are listed in Table 2 versus tolerance values.

Table 1: High Order Multipoles in Sextupole Magnets

Multipole	Measured	Tolerance
Normal 8-pole	$1.6e^{-4}$	$1e^{-1}$
Normal 10-pole	$1.3e^{-4}$	$1e^{-1}$
Normal 18-pole	$0.6e^{-4}$	$2e^{-3}$
Normal 30-pole	$0.1e^{-4}$	$1e^{-3}$
Skew 8-pole	$1.7e^{-4}$	$1e^{-1}$
Skew 10-pole	$1.0e^{-4}$	$1e^{-1}$

CONCLUSION

Results of magnetic measurement are within the SESAME machine tolerances mainly when *optimized alignment* is introduced to the dipoles whose out of specs gradient errors nonetheless can be compensated by quadrupoles. The beam dynamics is negligibly affected by the measured magnetic errors.

REFERENCES

[1] J. Marcos, V. Massana, J. Campmany, A. Milanese, C. Petrone, L. Walckiers, Proceedings of IPAC16.

[2] A. Milanese, E. Huttle, M. Shehab, IPAC14.

[3] M. Attal, E. Huttel, J.P. Koutchouk, Tech. Note SES-TE-AP-SPC-0002.

[4] M. Attal, E. Huttel, Proceedings of IPAC14.

[5] ZHANG Man-Zhou et al, Chinese Physics C (HEP & NP), Vol. 32, No. 11, Nov. 2008.

[6] A. Terebilo, SLAC-PUB-8732.

[7] BETA, J. Payet. CEA/DSM/ Irfu/ SACM, ftp:// ftp.cea.fr/incoming/y2k01/beta/.